Journal of
Manufacturing and Materials Processing

MDPI

Article

Thermal Management of Friction-Drilled A356 Aluminum Alloy: A Study of Preheating and Drilling Parameters

Ahmed Abdalkareem [1], Rasha Afify [1], Nadia Hamzawy [1], Tamer S. Mahmoud [1] and Mahmoud Khedr [1,2,*]

[1] Mechanical Engineering Department, Faculty of Engineering at Shoubra, Benha University, Cairo 11629, Egypt
[2] Future Manufacturing Technologies (FMT), Kerttu Saalasti Institute, University of Oulu, Pajatie 5, FI-85500 Nivala, Finland
* Correspondence: mahmoud.khedr@feng.bu.edu.eg or mahmoud.khedr@oulu.fi

Abstract: Friction drilling is a non-conventional process that generates heat through the interaction between a rotating tool and a workpiece, forming a hole with a bushing. In this study, the effect of the preheating temperature, rotational speed, and feed rate on the induced temperature during the friction drilling of A356 aluminum alloy was investigated. This study aimed to analyze the influence of friction-drilling parameters on the thermal conditions in the induced bushing, where it focused on the relationship between preheating and the resulting heat generation. The analysis of variance (ANOVA) approach was carried out to optimize the friction-drilling parameters that contributed most to the induced temperature during the friction-drilling processing. Experiments were conducted at various preheating temperatures (100 °C, 150 °C, 200 °C), rotational speeds (2000 rpm, 3000 rpm, 4000 rpm), and feed rates (40 mm/min, 60 mm/min, 80 mm/min). The induced temperature during the process was recorded using an infrared camera, where the observed temperatures ranged from a minimum of 154.4 °C (at 2000 rpm, 60 mm/min, and 100 °C preheating) to a maximum of 366.8 °C (at 4000 rpm, 40 mm/min, and 200 °C preheating). The results show that preheating increased the peak temperature generated in the bushing during friction drilling, especially at lower rotational speeds. The rotational speed rise led to an increase in the induced temperature. However, the increase in the feed rate resulted in a decrease in the observed temperature. The findings provide insights into optimizing friction-drilling parameters for enhanced thermal management in A356 aluminum alloy.

Keywords: friction drilling; bush temperature; infrared camera; ANOVA; Pareto analysis; optimization

Citation: Abdalkareem, A.; Afify, R.; Hamzawy, N.; Mahmoud, T.S.; Khedr, M. Thermal Management of Friction-Drilled A356 Aluminum Alloy: A Study of Preheating and Drilling Parameters. *J. Manuf. Mater. Process.* **2024**, *8*, 251. https://doi.org/10.3390/jmmp8060251

Academic Editor: Edouard Rivière-Lorphèvre

Received: 17 October 2024
Revised: 5 November 2024
Accepted: 6 November 2024
Published: 8 November 2024

Copyright: © 2024 by the authors. Licensee MDPI, Basel, Switzerland. This article is an open access article distributed under the terms and conditions of the Creative Commons Attribution (CC BY) license (https://creativecommons.org/licenses/by/4.0/).

1. Introduction

Friction drilling is a cutting-edge manufacturing technique that has revolutionized hole-making processes, especially in thin-walled materials, such as aluminum alloys [1]. It is also known as thermal drilling, form drilling, or flow drilling. This non-conventional drilling process is preferred for soft materials, such as aluminum alloys, to avoid the formation of cracks in the produced bushing [2]. Unlike conventional drilling, where material is removed to create a hole, friction drilling uses a specially designed tool rotating at high speeds to generate sufficient thermal energy through friction [3]. This heat softens the material, allowing it to deform plastically without chip production, thus creating a hole and simultaneously forming a bushing around the hole's edge [4]. The bushing created through this process enhances the structural integrity of the material, allowing for improved load-bearing capacities without the need for additional fasteners [5,6].

The friction-drilling process is especially beneficial in reducing the manufacturing steps, as it eliminates the need for operations such as nut welding or riveting insertion [7]. The process strengthens the hole by forming a bushing, providing better thread

engagement and improved load-bearing capabilities, making it highly suitable for industries, like the automotive, aerospace, and electronics industries [8,9]. The resulting bushing is typically two to three times the thickness of the original sheet material, enabling thin sheets to be used for threaded connections without compromising the strength [10].

Despite its advantages, friction drilling generates significant heat during the process, which can influence both the quality of the hole and the durability of the tool [11]. The induced temperature plays a crucial role in the formation of bushings because it influences the material flow during processing [5]. Previous studies showed that the friction-drilling process results in the formation of three distinct zones: the stir zone (SZ), the thermomechanically affected zone (TMAZ), and the heat-affected zone (HAZ) [12,13]. These zones are influenced by the heat generated during the process, and controlling the induced temperature is essential to optimizing the hole quality and extending the tool life.

Research showed that aluminum exhibits varying thermal responses during friction drilling. For example, Eliseev et al. [14] and Miller et al. [15] investigated the peak temperatures in the friction drilling of different aluminum alloys, finding that rotational speed and feed rate significantly impact the peak temperatures. During the friction drilling of 6082 aluminum alloy, the peak temperatures can range from 220 °C to 380 °C, depending on process parameters [5,16]. This thermal management challenge becomes even more pronounced in A356 aluminum alloy, known for its brittleness in the as-cast condition [17], making it necessary to control the heat generated during the drilling process to avoid overheating and damaging the material.

One promising approach to controlling heat generation during friction drilling is preheating the workpiece. Preheating softens the material, allowing the friction-drilling tool to penetrate more smoothly and reducing the overall thermal stress on both the tool and the workpiece [18]. Therefore, the technique of preheating the material before the drilling process can lower its initial resistance to the plastic deformation, increasing the peak temperatures generated during the drilling process, and consequently, decreasing petal formation. However, the effects of preheating, in combination with other critical parameters, like the rotational speed and feed rate, on the induced temperature during friction drilling of A356 aluminum alloy have not been comprehensively studied.

In the present study, the effect of preheating, along with variations in the rotational speed and feed rate, on the induced temperature during the friction drilling of A356 aluminum alloy were investigated. This study presented an optimization of the friction-drilling parameters by controlling the heat generation to improve the hole quality, reduce the tool wear, and enhance the bushing formation through the analysis of variance (ANOVA) approach. By understanding how preheating influences the thermal environment during friction drilling, this study contributed to optimizing the process parameters for A356 aluminum alloy, a widely used material in industrial applications requiring lightweight and corrosion resistance, such as housing covers [17].

Unlike traditional friction-drilling studies, which typically examine friction-generated temperatures alone, this research evaluated how preheating at multiple levels affected the temperature variation and tool–material interactions. This dual-temperature approach allowed for a more comprehensive understanding of the thermal response in aluminum alloys during friction drilling in the as-cast condition through the exploration of preheating temperatures (100 °C, 150 °C, 200 °C) and their interactions with rotational speeds (2000–4000 rpm) and feed rates (40–80 mm/min). Through this investigation, we aimed to provide insights into the thermal management of friction drilling A356 Al-alloy, leading to improved process efficiency and material performance for industrial applications requiring lightweight, high strength, and good corrosion resistance properties.

2. Experimental Methodology

2.1. Production of As-Cast Sheets

The present study investigated the friction drilling of as-cast 356 Al alloy. The chemical composition of the material was as follows: 6.23 wt.% Si, 0.337 wt.% Mg, 0.136 wt.% Ti, 0.067 wt.% Fe, 0.0029 wt.% Mn, 0.004 wt.% Cu, 0.0007 wt.% Zn, and Bal. wt.% Al.

Commercial ingots of A356 Al-alloy were produced by the aluminum company of Egypt (Egyptalum, Cairo, Egypt). The ingots were melted in an induction furnace, as depicted in Figure 1a. After the melting, degassing was carried out via blowing argon gas in the ladle/crucible to avoid porosity formation [19]. Subsequently, the degassed melt was poured into a rectangular C-steel mold with dimensions of 200 × 50 × 50 mm^3, as displayed in Figure 1b. After the solidification, an electro-discharge machine (EDM) was used to cut square sheet layers with approximately 3 mm thickness and a side length of 50 mm, as displayed in Figure 1c. The produced sheets were ground by sandpapers (180, 500, and 800 grits) to obtain smooth surfaces.

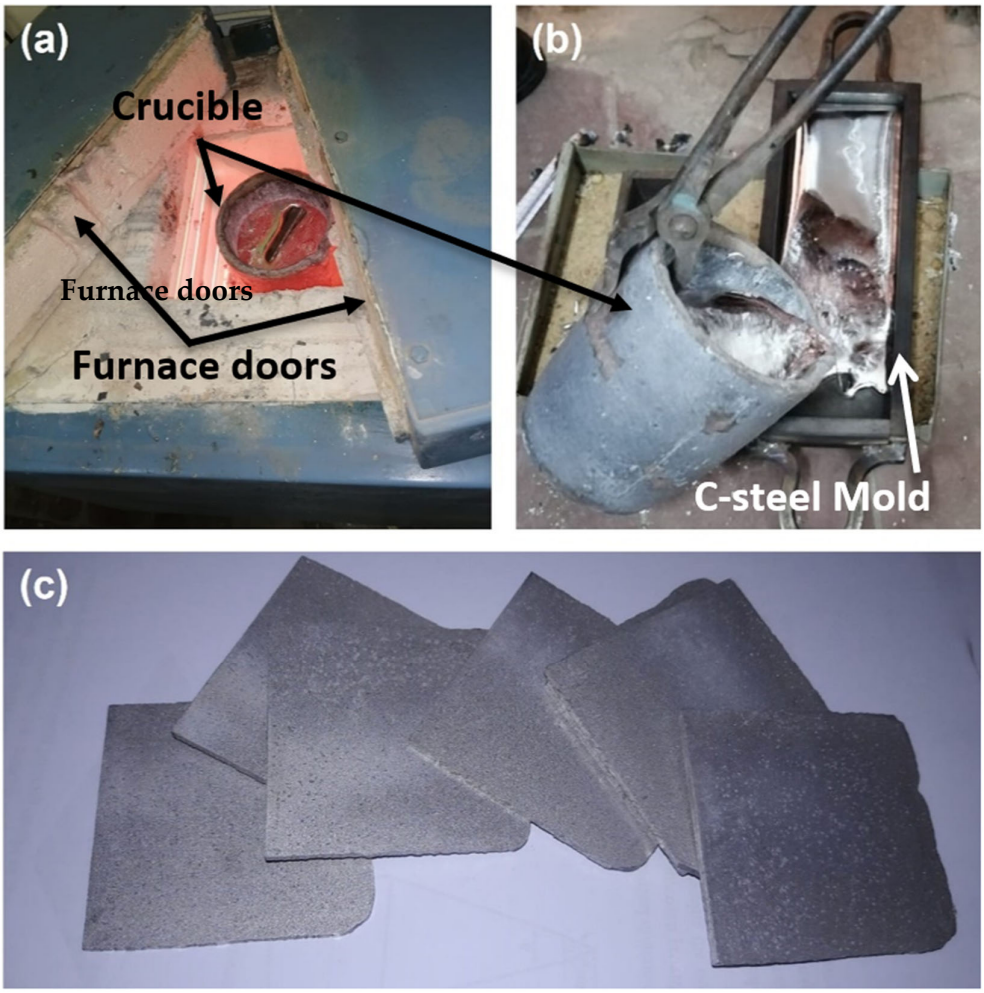

Figure 1. Preparation steps of the A356 Al-alloy sheet plates: (**a**) the as-received ingot melted in an electrical furnace, (**b**) the molten metal poured inside the steel mold, and (**c**) the sheet plates cut by EDM.

2.2. Friction-Drilling Tool

Figure 2 shows the dimensions, terminology, and geometry of the employed friction-drilling tool. It depicts a conical region of 7 mm depth and a cone angle of 58°. The

cylindrical region had a diameter of 10 mm, whereas the shoulder had a 20 mm diameter. The shank region, which was fixed in the spindle, had a diameter of 10 mm. The material of the utilized drilling tool was cold-rolled K100 steel, which has good wear resistance properties.

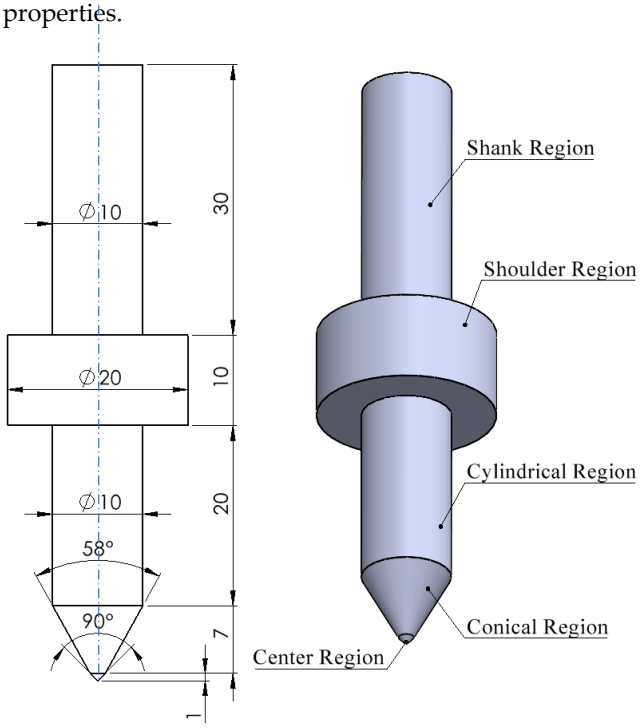

Figure 2. Schematic drawing representing the geometry and regions of the thermal drilling tool.

2.3. Preheating Adjustments

The processed sheets were placed in an electric furnace (Nabertherm B180, Lilienthal, Germany) for the preheating stage. The furnace was heated to temperatures of 100 °C, 150 °C, and 200 °C individually, according to the experimental condition. To account for potential heat loss, the furnace was extra-heated to 35 °C above the test temperature before placing the samples in the center of the furnace and held for 5 min until reaching the required temperature. The preheating took approximately 1 min before the drilling operation started (the time between moving the sample from the furnace and placing it inside the fixture). Note that preheating was applied before the drilling process and was not maintained continuously during drilling; therefore, the temperature increase during drilling was primarily due to the frictional heat generated by the tool–material interaction. While higher preheating temperatures (such as 300 °C and 400 °C) may further facilitate material deformation, they were not included in this study to avoid excessive thermal softening, which could compromise the structural integrity of the A356 Al alloy.

2.4. Friction-Drilling Processing

A PRATIC PB-20 three-axis vertical milling machine was utilized for the friction-drilling processes for A356 aluminum sheets. Figure 3 shows the milling machine and the fixation setup of the workpiece to ensure the sheet did not move during the drilling process, which could result in inaccuracies of the produced holes. The drilling conditions involved different parameters, namely, various spindle speeds (2000, 3000 and 4000 rpm), tool feed rates (40, 60, and 80 mm/min), and workpiece preheating temperatures (100, 150, and 200 °C). The drilling parameters were selected according to the literature [20,21].

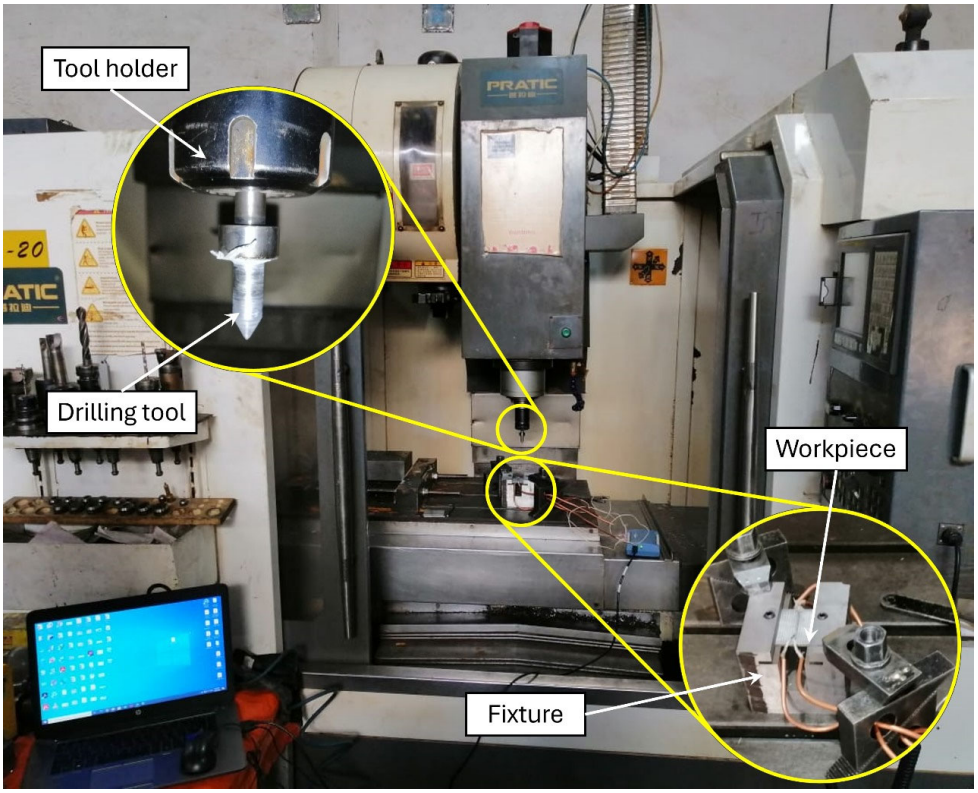

Figure 3. The CNC vertical milling machine used to accomplish the friction-drilling processes is represented with a magnified image of the fixture, tool, and workpiece.

2.5. Temperature Recording

A thermal imager (FLUKE Ti32) infrared camera with a resolution of 240 × 180 pixels was applied to measure the generated temperature between the friction-drilling tool and the workpiece. The camera was placed at approximately 0.5 m away from the tool/workpiece interface during the friction-drilling processing.

2.6. Experimental Factors and Levels

The tool rotational speed, feed rate, and workpiece preheating temperature were the key friction-drilling parameters considered in this study. A systematic approach using design of experiments (DOE) was employed to optimize the experimental plan and explore the interactions between the drilling parameters [22]. The investigation was conducted within a predetermined range of values for these parameters, as presented in Section 2.4. A full factorial design, a branch of DOE methodology, was employed to ensure that all possible combinations of the selected parameters were tested. This method allows for a thorough investigation of the main effects of each factor, as well as their interactions. Table 1 presents the design levels that corresponded to the thermal drilling parameters used in the experiments. With three factors at three levels, the experimental design required a total of 27 experimental runs (3 levels per factor, $3^3 = 27$).

Table 1. Mapping design levels of friction-drilling parameters.

Drilling Parameters	Rotational Speed (rpm)	Feed Rate (mm/min)	Preheating Temperature (°C)
Level 1	2000	40	100
Level 2	3000	60	150
Level 3	4000	80	200

3. Results and Discussion

3.1. Evolution of the Induced Temperature During Friction Drilling

Figure 4 shows a thermal image as obtained through the infrared camera and captured before starting the thermal drilling operation of a specimen preheated at 200 °C. It displays temperature variations across the friction-drilling tool, workpiece, and surroundings. The highest recorded temperature was approximately 212 °C, which was the temperature of the preheated workpiece after its insertion in the fixture, just before starting the drilling processing. The lowest temperature in the image was approximately 22 °C, which was observed at a location further from the drilling zone and represented the ambient temperature of the surroundings. The temperature distribution is visually represented through a color gradient, with warmer areas depicted in bright yellow and cooler regions in purple, providing a clear contrast of temperature distributions. This thermal analysis of the working temperature underscores the critical importance of managing heat during the drilling process to avoid material adhering to the drilling tool and ensure optimal machining conditions.

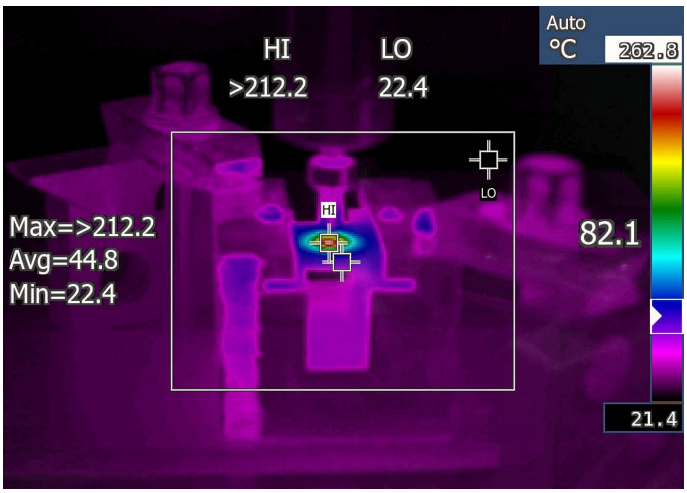

Figure 4. A thermal image captured via the infrared camera displaying the temperature distribution of a specimen preheated at 200 °C before the friction-drilling processing.

Figure 5 presents the temperature distributions during the friction-drilling processing of the A356 aluminum alloy at a rotational speed of 4000 rpm, a feed rate of 60 mm/min, and a preheating temperature of 200 °C. Figure 5a shows the initial temperature distribution of the workpiece prior to the tool penetration. At this stage, the rotating tool was positioned above the workpiece, with its tip aligned at the intended drilling location, but no material penetration had occurred. The downward axial force, governed by the feed rate, drove the tool toward the workpiece. It is important to note that the experiment commenced only after the sample reached the targeted preheating temperature, with a slight overshoot of approximately 10 °C.

In Figure 5b, the temperature distribution is illustrated after the immediate contact between the tools and the workpiece. The friction between the rotating tool and the aluminum sheet generated substantial heat, which caused the material in the contact area to soften. The maximum temperature observed under these drilling conditions was 344.7 °C. At this stage, the tool's conical section, combined with the applied axial force, induced plastic deformation in the material without producing chips, as the softened material flowed rather than being cut. The temperature distribution was concentrated around the conical region, where the material was being softened and deformed.

Figure 5c depicts the temperature change as the tool continued to penetrate the specimen and went deeper through it. As the tool penetrated deeper, the softened material

flowed radially outward from the center. The maximum observed temperature decreased to 200.9 °C as the generated heat began to diffuse into the surrounding workpiece. The shoulder of the tool also contributed by generating heat as it came into contact with the material's surface. Here, the temperature was primarily concentrated in the conical and shoulder regions due to the constant contact between the tool and the workpiece.

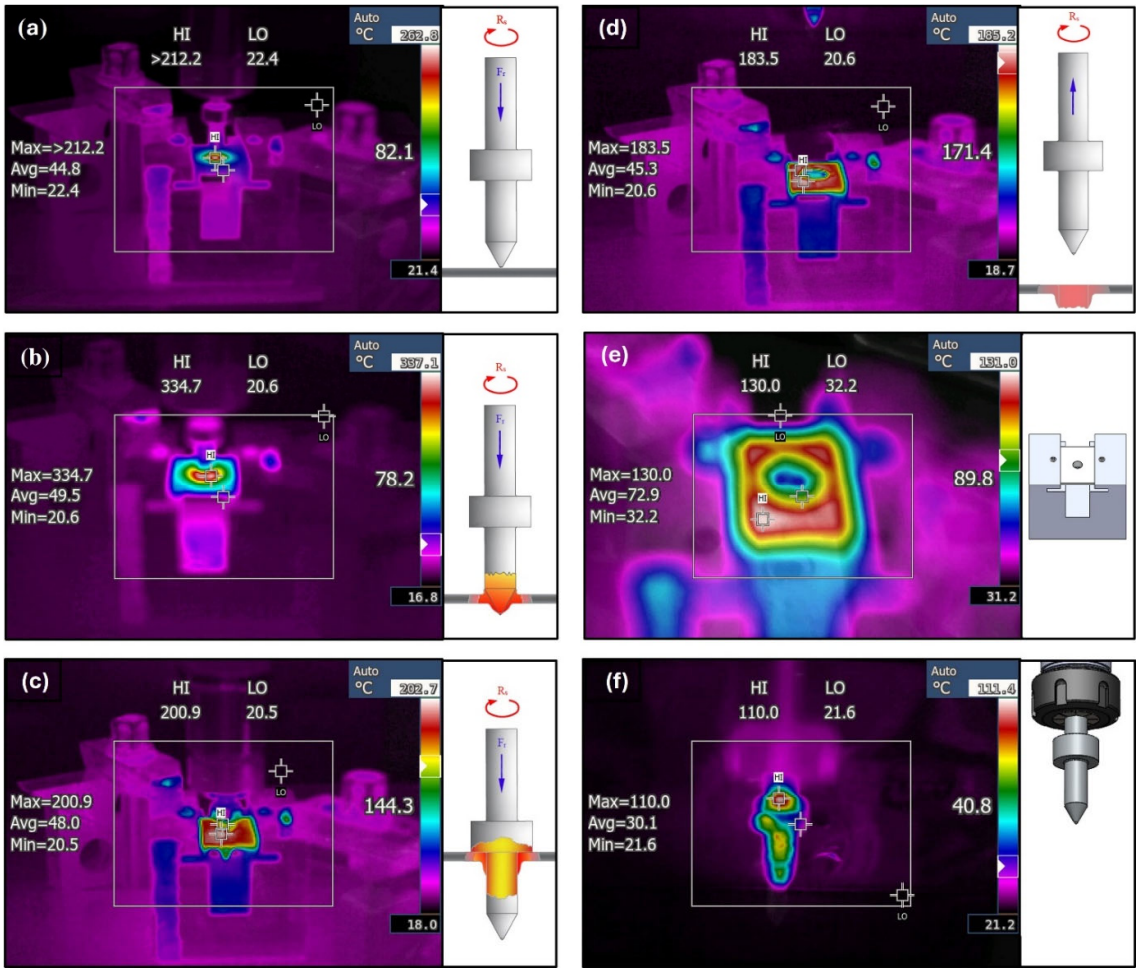

Figure 5. Temperature recording and distribution during the friction-drilling stages under working conditions of a rotational speed at 4000 rpm, a feed rate of 60 mm/min, and preheating temperature of 200 °C: (**a**) centering, (**b**) tool penetration, (**c**) processing of the hole, (**d**) the tool-retracting stage, (**e**) complete bushing formation, and (**f**) tool removal.

Figure 5d demonstrates the temperature distribution at the end of the drilling process. Once the tool retracted from the workpiece, the frictional heat generation ceased, and the temperature began to decrease. However, the material around the newly formed hole remained hot for a brief period as the heat dissipated into the surrounding material, the drilling tool, and the ambient air. Some of the generated heat was retained in the tool, which gradually cooled down with the aid of external cooling air.

Figure 5e highlights the temperature dissipation in the workpiece after the drilling process, where the temperature decreased to 130 °C. The reduction in the temperature was due to heat dissipation through two main mechanisms: external cooling from the contact between the workpiece and the fixture, and internal cooling from the air contact within the drilled hole.

Finally, Figure 5f depicts the temperature distribution in the tool after the friction-drilling process. A maximum temperature of 110 °C was recorded on the tool surface,

primarily due to the adhesion of the aluminum alloy onto the tool's cylindrical and shoulder regions. This material adhesion is a critical factor that affects tool performance, as it alters the tool's geometry, leading to potential inconsistencies in hole formation, dimensional inaccuracies, and uneven tool wear. Additionally, the accumulation of the adhesive material may act as a thermal barrier, affecting the tool's initial temperature during subsequent drilling operations and impeding the uniform distribution of heat across the workpiece during the drilling process.

Figure 6 depicts a bar chart of the relationship between the tool rotational speed, feed rate, and preheating temperature on the maximum induced temperatures measured during the friction-drilling process. The data are presented for three distinct preheating temperature levels: 100 °C, 150 °C, and 200 °C, represented by blue, red, and green bars, respectively. The experiments were performed at three feed rates: 40 mm/min, 60 mm/min, and 80 mm/min, with spindle speeds that ranged from 2000 rpm to 4000 rpm. At a preheating temperature of 100 °C, the chart reveals a steady increase in the induced temperature as the rotational speed increased from 2000 rpm to 4000 rpm across all feed rates. For instance, at a feed rate of 40 mm/min, the induced temperature rose from approximately 166.5 °C at 2000 rpm to around 224.7 °C at 4000 rpm. A similar trend was observed at higher feed rates, where the temperatures reached 200.9 °C and 196.9 °C for the feed rates of 60 mm/min and 80 mm/min, respectively, with a rotational speed of 4000 rpm and preheating at 100 °C.

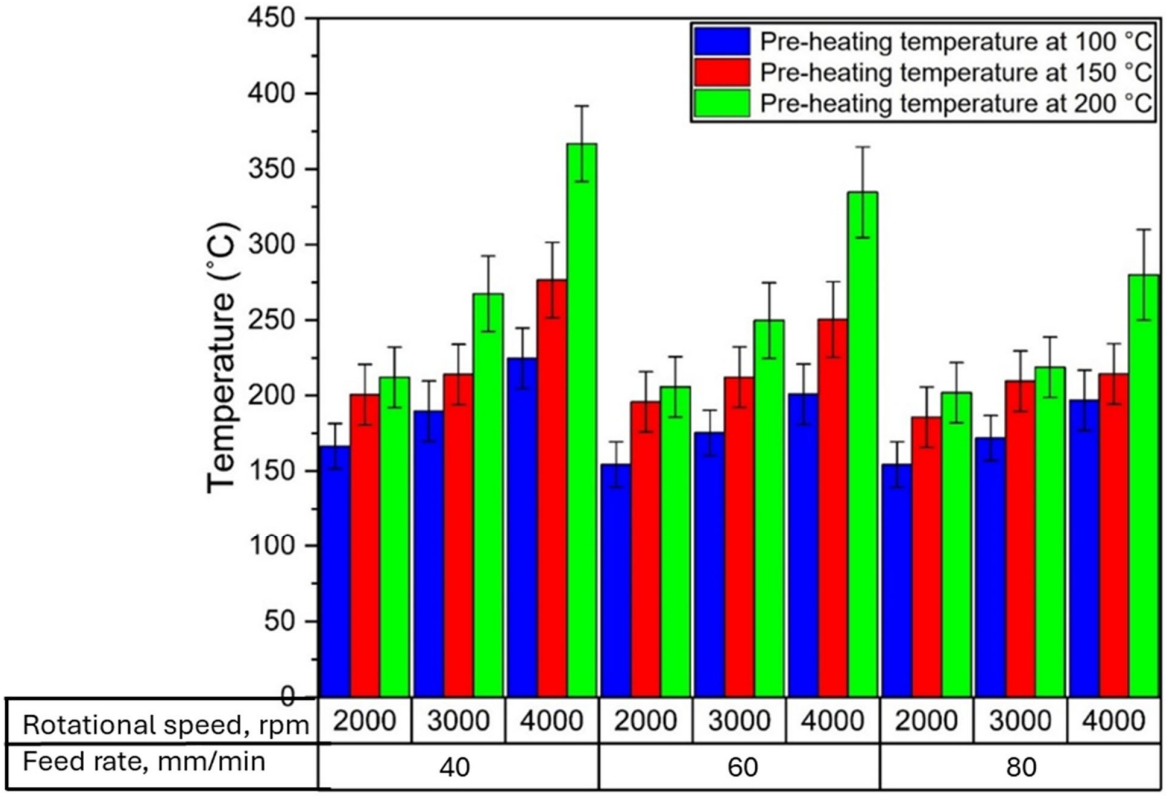

Figure 6. The maximum induced temperature at the tool/workpiece interface during the friction drilling of A356 Al alloy at different preheating temperatures, rotational speeds, and feed rates.

Figure 6 also highlights that the maximum induced temperature occurred at the lowest feed rate of 40 mm/min. At this constant feed rate, the temperature consistently increased as both the preheating temperature and spindle speed rose. When the preheating temperature was increased to 150 °C, the induced temperature became more pronounced, where it reached approximately 276.5 °C at the highest spindle speed of 4000 rpm. This

trend continued at the highest preheating temperature of 200 °C, where the maximum induced temperature peaked at 366.8 °C at 4000 rpm.

The results underscore a clear relationship between the preheating temperature, spindle speed, and feed rate. Higher preheating temperatures consistently led to higher induced temperatures across all feed rates and spindle speeds. Similarly, an increased spindle speed resulted in higher temperatures, an effect that was further amplified as both the preheating temperature and feed rate increased, in agreement with the literature [23,24]. These findings suggest that temperature control during the friction-drilling process was highly dependent on these variables, with each playing a critical role in influencing the overall thermal behavior during the friction drilling of the A356 Al alloy. However, we needed to analyze which parameter contributed the most to the thermal management during the friction-drilling processing, which is discussed in the following section.

3.2. Optimization of Friction-Drilling Parameters

This section evaluates the adequacy of the results and presents a mathematical model developed through regression analysis to predict the effects of the selected control factors (rotational speed, feed rate, and preheating temperature) on the output response, i.e., the induced temperature. The relationships between these factors and the output response were analyzed using ANOVA and main effect plots. ANOVA is a statistical tool used to break down the total variability in the data into components attributed to specific sources of variation, enabling hypothesis testing about the model's parameters [25]. In this study, ANOVA was employed to assess the relative effects of the different process parameters on the observed temperatures. Additionally, a Pareto analysis was conducted to further investigate the contributions of the statistically significant factors [26].

To evaluate the performance of the regression model, the ANOVA results were scrutinized, with particular attention given to the Prob > F values. In this context, a Prob > F value less than 0.05 indicated that the corresponding model term was statistically significant at a 95% confidence level [25]. Table 2 provides a summary of the ANOVA results for the observed temperatures, demonstrating that the developed regression model was well suited for predicting the temperatures during the friction drilling of the A356 aluminum alloy. The model's R-squared (R^2) value was found to be 87.3%, suggesting that the independent variables (rotational speed, feed rate, and preheating temperature) explained a substantial portion of the total variation in the observed temperature. This indicates that the model provided a strong fit to the experimental data. The percentage contribution (PC) of each process parameter to the observed temperature was calculated using the formula

$$PC = \frac{SS_d}{SST}$$

where SS_d is the sum of the squared deviations for a specific parameter, and SST is the total sum of the squares, representing the total variation in the data.

As presented in Table 2, the preheating temperature contributed 41.56% to the observed temperature, making it the most influential factor in the process with minimal variation. In contrast, the feed rate exhibited a lower percentage contribution of 6.81%, indicating that it had a lesser impact on the observed temperature and was associated with higher variation. The spindle speed also played a significant role, but its contribution was intermediate between the preheating temperature and feed rate. These results suggest that the preheating temperature was the most critical factor in controlling the induced temperature during the friction-drilling process, followed by the spindle speed, while the feed rate had a relatively smaller influence.

Overall, the findings underscore the importance of optimizing the preheating temperature and spindle speed to achieve the desired thermal conditions in the drilling process, while the feed rate adjustments had a more modest effect on the temperature control.

Table 2. Analysis of variance for the recorded temperature during friction drilling.

Source	DF	Adj SS	Adj MS	F-Value	*p*-Value	P_c
Linear	6	57,532	9588.7	22.33	0.000	
Rotational speed, rpm	2	25,547	12,773.5	29.74	0.000	38.64%
Feed rate, mm/min	2	4507	2253.5	5.25	0.015	6.81%
Preheating temperature, °C	2	27,478	13,739.0	31.99	0.000	41.56%
Error	20	8590	429.5	R-sq = 87.01	Rs-(adj) = 83.11	12.99%
Total	26	66,122				100%

Figure 7a illustrates the main effect plots for the response variable, i.e., the maximum induced temperature during friction drilling (observing temperature). The plot clearly shows that the mean induced temperature increased with higher rotational speeds and preheating temperatures. This increase in the rotational speed led to greater frictional heat generation due to the intensified contact between the tool and the workpiece. Conversely, an increase in the feed rate from 40 mm/min to 80 mm/min resulted in a reduction in the induced temperature by approximately 35 °C. This decrease occurred because the higher feed rates reduced the contact time between the tool and the workpiece, which lowered the amount of frictional heat generated during the process. The main effects plot highlights the optimal combination of machining parameters for achieving the highest induced temperature during the friction drilling. The optimal parameters were identified as rotational speed (RS) = 4000 rpm, feed rate = 40 mm/min, and preheating temperature = 200 °C. These conditions resulted in the highest maximum generated temperatures, indicating the most efficient thermal management during the process.

To further validate the significance of each factor, a Pareto chart, presented in Figure 7b, was employed to identify the most important contributors to the induced temperature. As shown in Figure 7b, the preheating temperature emerged as the most influential factor, with approximately 41%, followed by the rotational speed and feed rate with approximately 39%. This analysis confirmed that the preheating temperature had the greatest effect on the thermal conditions during the friction drilling, while the rotational speed also played a critical role, whereas the feed rate had a relatively smaller impact.

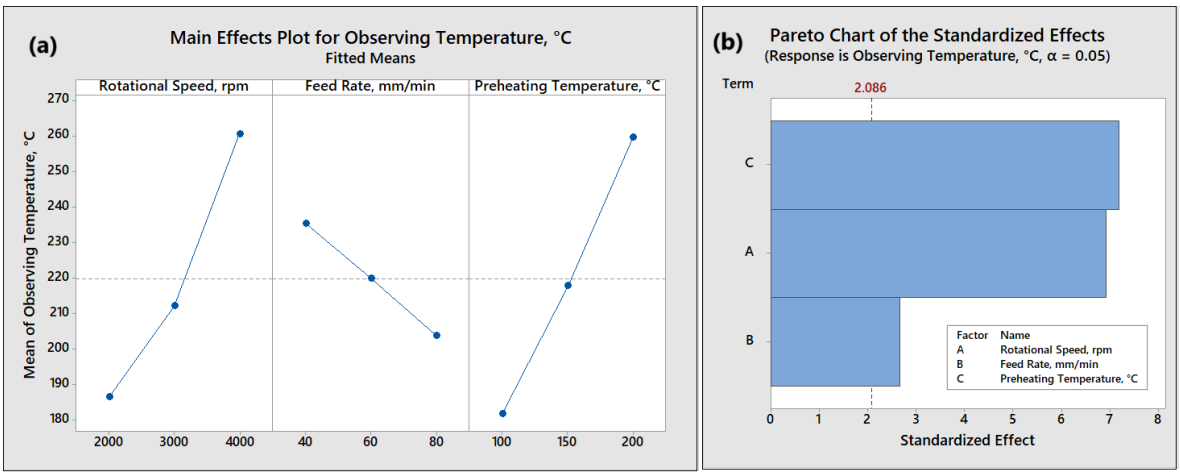

Figure 7. (**a**) Main effects plots and (**b**) Pareto chart of the friction-drilling parameters affecting the observing temperature in the produced bushings.

Figure 8 presents a normal probability plot of the fitted and residual data to evaluate the normality of the residuals, which is crucial for assessing the normality of the response

data. The residuals represent the difference between the observed values and the predicted (or fitted) values from the model. In the normal probability plot, if the points approximately followed a straight line, this indicates that the residuals were normally distributed. A straight-line pattern in the plot confirmed that the residuals conformed to the assumptions of normality, which was important for validating the linear model [27]. Additionally, the versus fits plot shows the residuals plotted against the fitted values. This plot was used to detect patterns, such as heteroscedasticity, which referred to non-constant variance in the residuals. In this case, the points in the versus fits plot appeared to be randomly scattered around the horizontal line at zero, suggesting that there was no clear pattern or evidence of heteroscedasticity.

Based on the analysis of these residual plots, the model satisfied the assumptions of normality, homoscedasticity (constant variance), and independence. The normal probability plots and residual analysis demonstrated that the regression model adhered to the assumptions of normality, homoscedasticity, and independence. The residuals were randomly distributed, with no evidence of heteroscedasticity or autocorrelation, which ensured the robustness of the model. However, we recommend providing a larger dataset to improve the output response of the ANOVA approach and achieve more robust statistical conclusions in future works. Furthermore, we recommend the investigation of surface conditions of the formed bushing for future studies to provide valuable insights into the tool–material interaction and assess the overall quality of the bushing formed through friction drilling assisted by preheating.

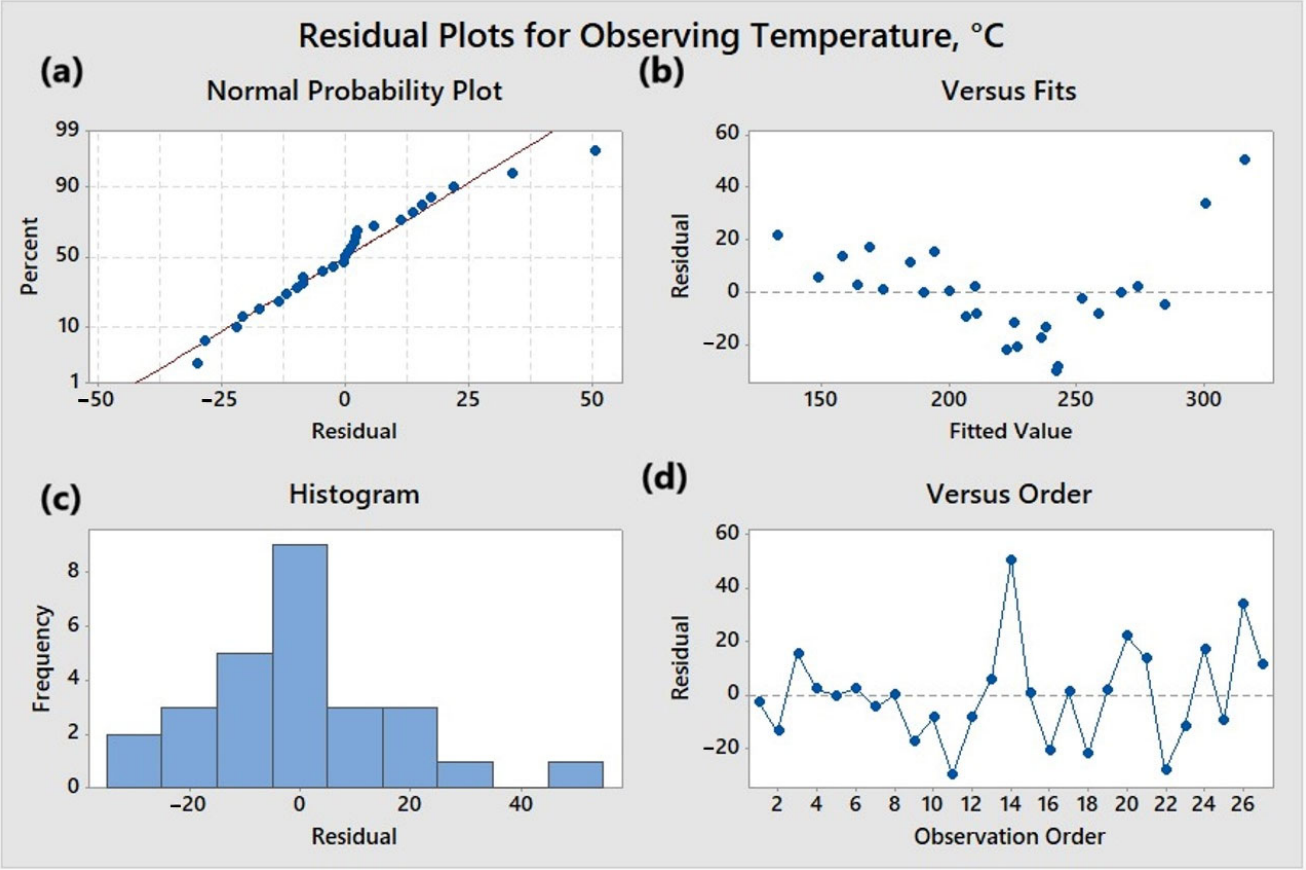

Figure 8. Normal probability plot and residual graphs: (**a**) normal probability plot for residuals, (**b**) residuals vs. fitted values, (**c**) histograms of residuals, and (**d**) residuals vs. the order of the data.

4. Conclusions

In the current work, temperature variations during the friction drilling of as-cast A356 Al alloy were observed under different conditions, namely, preheating temperatures (100, 150, and 200 °C), rotational speeds (2000, 3000, and 4000 rpm), and feed rates (40, 60, and 80 mm/min). A series of experiments were carried out to investigate the drilling parameters' effects on the induced temperature in the formed bushings. The main findings of this study were as follows:

1. Preheating temperature emerged as the most significant factor that influenced the induced temperature during the friction-drilling process. Higher preheating temperatures consistently resulted in increased induced temperatures, with a maximum recorded value of 366.8 °C at a preheating temperature of 200 °C, spindle speed of 4000 rpm, and feed rate of 40 mm/min. This indicates that preheating was a critical parameter for thermal management in the process.
2. The rotational speed also played a significant role in increasing the induced temperature. As the spindle speed increased from 2000 rpm to 4000 rpm, the temperature rose proportionally. The combination of high spindle speed and high preheating temperature produced the highest levels of heat during the friction drilling, which contributed to the efficiency of the process in terms of the material flow and bushing formation.
3. The feed rate exhibited a smaller influence on the induced temperature compared with the preheating temperature and spindle speed. A lower feed rate of 40 mm/min resulted in the highest temperatures due to prolonged contact between the tool and the workpiece, which allowed more frictional heat to be generated. In contrast, higher feed rates reduced the induced temperature by limiting the time for heat generation during the drilling process.
4. The ANOVA results validated the statistical significance of the process parameters. The regression model demonstrated a high degree of fit, with an R^2 value of 87.3%, indicating that the chosen independent variables reasonably explained the variation in the induced temperature. The Pareto analysis further confirmed that the preheating temperature contributed 41.56% to the total variation, which made it the most influential factor, followed by the rotational speed at 38.64% and feed rate at 6.81%.

In summary, this study emphasized the critical role of the preheating temperature and rotational speed in optimizing the friction-drilling process for A356 aluminum alloy. By carefully adjusting these parameters, the thermal conditions can be managed to enhance the quality of the hole formation and reduce tool wear, leading to improved process efficiency and product performance. These findings provide a basis for further optimization and exploration of friction drilling in various industrial applications.

Author Contributions: A.A.: writing—original draft, data curation, validation, formal analysis, methodology, and investigation. R.A.: conceptualization, supervision, and writing—review and editing. N.H.: writing—original draft, investigation, validation, formal analysis, and review and editing. T.S.M.: conceptualization, supervision, and writing—review and editing. M.K.: writing—original draft, data curation, validation, formal analysis, methodology, investigation, conceptualization, supervision, and writing final draft—review and editing. All authors have read and agreed to the published version of this manuscript.

Funding: The authors acknowledge the financial support of the TeräsPuu and KV-Noste projects.

Informed Consent Statement: This research excluded human participants, their data, or biological material, and it also excluded animals.

Data Availability Statement: Data will be made available upon request.

Conflicts of Interest: The authors declare no conflicts of interest.

References

1. Khedr, M.; Hamzawy, N.; Jaskari, M.; Hamada, A.; Mahmoud, T.S.; El-Mahallawi, I.; Khalifa, T. Improved mechanical behavior of friction stir drilled 6082 aluminum alloy via T6 treatment. *J. Mater. Res. Technol.* **2024**, *31*, 2774–2785. https://doi.org/10.1016/j.jmrt.2024.06.189.
2. Krebs, C.; Heyser, D.; Schweizer, B.; Volz, M.; Abele, E.; Weigold, M. Numerical and experimental analysis of margin geometries of twist drills in deep hole machining operations. *Adv. Ind. Manuf. Eng.* **2023**, *6*, 100120. https://doi.org/10.1016/j.aime.2023.100120.
3. Heiler, R. Flow drilling technology and thread forming-an economical and secure connection in hollow sections and thin-walled components. *E3S WebConf. EDP Sci.* **2019**, *97*, 06033. https://doi.org/10.1051/e3sconf/20199706033.
4. Dehghan, S.; Soury, E.; Ismail, M.I.S.B. A comparative study on machining and tool performance in friction drilling of difficult-to-machine materials AISI304, Ti-6Al-4V, Inconel718. *J. Manuf. Process.* **2021**, *61*, 128–152. https://doi.org/10.1016/j.jmapro.2020.10.078.
5. Hamzawy, N.; Khedr, M.; Mahmoud, T.S.; et al. *Investigation of Temperature Variation During Friction Drilling of 6082 and 7075 Al-Alloys*; Min Metal Mater Soc (TMS): 471–477; Springer: Cham, Switzerland, 2020. https://doi.org/10.1007/978-3-030-36408-3_6.
6. Skovron, J.D.; Prasad, R.R.; Ulutan, D.; Mears, L.; Detwiler, D.; Paolini, D.; Baeumler, B.; Claus, L. Effect of Thermal Assistance on the Joint Quality of Al6063-T5A During Flow Drill Screwdriving. *J. Manuf. Sci. Eng.* **2015**, *137*, 051019. https://doi.org/10.1115/1.4031242.
7. Mutalib, M.Z.A.; Ismail, M.I.S.; Jalil, N.A.A.; As'arry, A.J.J.T. Characterization of tool wear in friction drilling. *J. Tribol.* **2018**, *17*, 93–103.
8. Wu, H.; Clarke, R.; Porter, M.; Ward, R.; Quinn, J.; McGarrigle, C.; McFadden, S. Thread-stripping test procedures leading to factors of safety data for friction-drilled holes in thin-section aluminium alloy. *Thin-Walled Struct.* **2021**, *163*, 107653. https://doi.org/10.1016/j.tws.2021.107653.
9. Yashar, S.; Sarafraz, Y.; Alexander, K.; Felinks, N.; Dirk, B.; Frank, W. Influence of pre-drilling on hardness and tensile failure of formed internal threads in thin-walled AZ91 cast alloys. *Eng. Fail. Anal.* **2021,** *130***,** 105783. https://doi.org/10.1016/j.engfailanal.2021.105783.
10. Waleed, W.A.; Chathriyan, A.; Singh Sam, R.V.; Singh Vimal, S. Experimental investigation on the influence of process parameters in thermal drilling of metal matrix composites. *FME Trans.* **2018**, *46*, 171–176. https://doi.org/10.5937/fmet1802171w.
11. Mathew, A.; Raja, V.K.B.; Palanikumar, K.; Sanjay, D.R.S.K.; Subbaiah, B.V.; Chandra, L.V.R. Highlights of Non-traditional friction drilling process A review. *Mater. Today Proc.* **2021**, *46*, 3582–3587. https://doi.org/10.1016/j.matpr.2021.01.336.
12. Bustillo, A.; Urbikain, G.; Perez, J.M.; Pereira, O.M.; de Lacalle, L.N.L. Smart optimization of a friction-drilling process based on boosting ensembles. *J. Manuf. Syst.* **2018**, *48*, 108–121. https://doi.org/10.1016/j.jmsy.2018.06.004.
13. Vanhove, H.; Ozden, E.; Duflou, J.R. An Experimental Study on Bushing Formation during Friction Drilling of Titanium Grade 2 for Medical Applications. *J. Manuf. Mater. Process.* **2023**, *7*, 220. https://doi.org/10.3390/jmmp7060220.
14. Eliseev, A.A.; Fortuna, S.V.; Evgeny, K.; Kalashnikova, T.A.; Kalashnikova, T.A. Microstructure modification of 2024 aluminum alloy produced by friction drilling. *Mater. Sci. Eng. A-Struct. Mater. Prop. Microstruct. Process.* **2017**, *691*, 121–125. https://doi.org/10.1016/j.msea.2017.03.040.
15. Scott, F.M.; Albert, J.S. Thermo-Mechanical Finite Element Modeling of the Friction Drilling Process. *J. Manuf. Sci. Eng.-Trans. Asme* **2007**, *129*, 531–538. https://doi.org/10.1115/1.2716719.
16. Ozek, C.; Demir, Z. Investigate the friction drilling of aluminum alloys according to the thermal conductivity. *Tem J.* **2013**, *2*, 93–101.
17. Albarbary, H.Y.E.; Afify, R.; Mansour, E.H.; Mahmoud, T.S.; Khedr, M. The effect of pre-drilling on the characteristics of friction drilled A356 cast aluminum alloy. *J. Manuf. Process.* **2022**, *82*, 646–656. https://doi.org/10.1016/j.jmapro.2022.08.040.
18. Guzanová, A.; Janoško, E.; Draganovská, D.; Vrabeľ, M.; Tomáš, M.; Horňak, P.; Vojtko, M.; Veligotskyi, N. Investigation of Applicability Flowdrill Technology for Joining Thin-Walled Metal Sheets. *Metals* **2022**, *12*, 540. https://doi.org/10.3390/met12040540.
19. Hamada, A.; Mansour, E.H.; Jaskari, M.; Abd-Elaziem, W.; Mohamed, A.K.; Elshokrofy, H.; Mustakangas, A.; Järvenpää, A.; Khedr, M. Strengthening aluminum matrix composite with additively manufactured 316L stainless steel lattice reinforcement: Processing methodology, mechanical performance and deformation mechanism. *J. Mater. Res. Technol.* **2024**, *29*, 1087–1101. https://doi.org/10.1016/j.jmrt.2024.01.172.
20. Sara Ahmed, E.-B. Pre-drilling Effect on Thermal Friction Drilling of Cast Aluminum Alloy Using Thermo-mechanical Finite Element Analysis. *Appl. Comput. Mech.* **2020**, *6*, 1371–1379. https://doi.org/10.22055/jacm.2020.34682.2455.
21. Demir, Z.; Özek, C. Investigate the Effect of Pre-drilling in Friction Drilling of A7075-T651. *Mater. Manuf. Process.* **2014**, *29*, 593–599. https://doi.org/10.1080/10426914.2014.892986.
22. Montgomery, D.C. *Design and Analysis of Experiments*, 3rd ed.; Ariz. Stat. Univ.: New York, NY, USA, 1991.
23. Su, K.-Y.; Welo, T.; Wang, J. Improving Friction Drilling and Joining through Controlled Material Flow. *Procedia Manuf.* **2018**, *26*, 663–670. https://doi.org/10.1016/j.promfg.2018.07.077.
24. Abbasi, R.; Dehghan, S.; Loh-Mousavi, M. Experimental investigation on friction drill joining of difficult-to-machine materials: A new methodology for joining of similar and dissimilar materials. *Weld. Int.* **2021**, *35*, 281–294. https://doi.org/10.1080/09507116.2021.1993108.

25. Hamzawy, N.; Mahmoud, T.S.; El-Mahallawi, I.; Khalifa, T.; Khedr, M. Optimization of Thermal Drilling Parameters of 6082 Al-Alloy Based on Response Surface Methodology. *Arab. J. Sci. Eng.* **2023**, *48*, 12001–12014. https://doi.org/10.1007/s13369-023-07628-9.
26. Bassiouny, N.A.; Al-Makky, M.; Youssef, H. Parameters affecting the quality of friction drilled holes and formed thread in austenitic stainless steel AISI 304. *Int. J. Adv. Manuf. Technol.* **2023**, *125*, 1493–1509.
27. Alphonse, M.; Bupesh Raja, V.K.; Gupta, M. Optimization of plasma nitrided, liquid nitrided & PVD TiN coated H13-D2 friction drilling tool on AZ31B magnesium alloy. *Mater. Today Proc.* **2021**, *46*, 9520–9528.

Disclaimer/Publisher's Note: The statements, opinions and data contained in all publications are solely those of the individual author(s) and contributor(s) and not of MDPI and/or the editor(s). MDPI and/or the editor(s) disclaim responsibility for any injury to people or property resulting from any ideas, methods, instructions or products referred to in the content.